Inorg. Chem. **XXXX**, *xx*, 0

Synthesis of Two New Linear Trinuclear Cu^{II} Complexes: Mechanism of Magnetic Coupling through Hybrid B3LYP Functional and CShM Studies

Santarupa Thakurta,[†] Joy Chakraborty,[†] Georgina Rosair,[‡] Javier Tercero,*[,§] M. Salah El Fallah,[§] Eugenio Garribba,[||] and Samiran Mitra*[,†]

Department of Chemistry, Jadavpur University, Raja S. C. Mullick Road, Kolkata 700 032, India, Department of Chemistry, School of Engineering & Physical Sciences, Heriot-Watt University, Edinburgh EH 14 4AS, U.K., Departament de Química Inorgànica, Facultat de Química, Universitat de Barcelona, Martí Franquès 1-11, 08028 Barcelona, Spain, and Department of Chemistry, University of Sassari, via Vienna 2, I-07100 Sassari, Italy

Received January 26, 2008

Two new Cu^{II} linear trinuclear Schiff base complexes, $[Cu_3(L)_2(CH_3COO)_2]$ (**1**) and $[Cu_3(L)_2(CF_3COO)_2]$ (**2**), have been prepared using a symmetrical Schiff base ligand H_2L [where H_2L = *N*,*N*′-bis(2-hydroxyacetophenone)propylenediimine]. Both of the complexes have been characterized by elemental analyses, Fourier transform IR, UV/vis, and electron paramagnetic resonance spectroscopy. Single-crystal X-ray structures show that the adjacent Cu^{II} ions are linked by double phenoxo bridges and a $\mu^2-\eta^1:\eta^1$ carboxylato bridge. In each complex, the central copper atom is located in an inversion center with distorted octahedral coordination geometry, while the terminal copper atoms have square-pyramidal geometry. Cryomagnetic susceptibility measurements over a wide range of temperature exhibit a distinct antiferromagnetic interaction of $J = -36.5$ and -72.3 cm^{-1} for **1** and **2**, respectively. Density functional theory calculations (B3LYP functional) and continuous-shape measurement (CShM) studies have been performed on the trinuclear unit to provide a qualitative theoretical interpretation of the antiferromagnetic behavior shown by the complexes.

Introduction

Schiff base complexes of transition metals have been widely employed in the development of heterogeneous catalysis,[1] molecular electronics, single-molecule-based magnetism, and photochemistry.[2–5] Their physical, optical, and electronic properties have been explored in different coordination environments with organic chelators, blockers, and suitable bridging units.[6–8] Exchange-coupled polynuclear Cu^{II} Schiff base complexes have gained particular attention because of their novel structural and magnetic properties, in addition to being considered as potential biomimic models for a number of key biosystems.[9,10] The H_2salen-type [*N*,*N*′-bis(salicylidene)ethane-1,2-diamine] Schiff bases have proved themselves as useful chelators in the synthesis of transition-metal complexes because of their synthetic accessibility, structural diversity and varied denticity.[11]

* To whom correspondence should be addressed. E-mail: smitra_2002@yahoo.com (S.M.), javier.tercero@qi.ub.es (J.T.).
[†] Jadavpur University.
[‡] Heriot-Watt University.
[§] Universitat de Barcelona.
[||] University of Sassari.

(1) Zhang, W.; Loebach, J. L.; Wilson, S. R.; Jacobsen, E. N. *J. Am. Chem. Soc.* **1990**, *112*, 2801.
(2) Cornils, B., Herrmann, W. A., Schlogl, R., Eds. *Catalysis from A−Z: A Concise Encyclopedia*; Wiley: New York, 2000.
(3) Farraro, J. R.; Williams, J. M. *Introduction to Synthetic Electrical Conductors*; Academic Press: New York, 1987.
(4) Miller, J. S., Drillon, M., Eds. *Magnetism: Molecules to Materials IV*; Wiley-VCH: Weinheim, Germany, 2003.
(5) (a) Marder, S. R., Sohn, J. E., Stucky, G. D., Eds. *Materials for Nonlinear Optics: Chemical Perspectives*; ACS Symposium Series; American Chemical Society: Washington, DC, 1991. (b) Evans, O. R.; Lin, W. *Acc. Chem. Res.* **2002**, *35*, 511.
(6) Karmakar, T. K.; Chandra, S. K.; Ribas, J.; Mostafa, G.; Lu, T. H.; Ghosh, B. K. *Chem. Commun.* **2002**, 2364, and references cited therein.
(7) Rahaman, S. H.; Bose, D.; Ghosh, R.; Fun, H.-K.; Ghosh, B. K. *Ind. J. Chem.* **2004**, *A43*, 11901.
(8) Bose, D.; Rahaman, S. H.; Mostafa, G.; Bailey Walsh, R. D.; Zaworotko, M. J.; Ghosh, B. K. *Polyhedron* **2004**, *23*, 545.
(9) (a) Snell, E. E.; Braunstein, A. E.; Severin, E. S.; Torchinsky, Y. M. *Pyridoxal Catalysis: Enzymes and Model Systems*; Interscience: New York, 1968. (b) Bkouche-Waksman, I.; Barbe, J. M.; Kvick, A. *Acta Crystallogr.* **1988**, *B44*, 595. (c) Krätsmar-Smogrovic, J.; Blahovà, M.; Kettmann, V. *Chirality* **1991**, *3*, 503.
(10) Apella, M. C.; Totaro, R.; Baran, E. J. *Biol. Trace Elem. Res.* **1993**, *37*, 293.
(11) Rahaman, S. H.; Ghosh, R.; Lu, T.-H.; Ghosh, B. K. *Polyhedron* **2005**, *24*, 1525.

10.1021/ic8001459 CCC: $40.75
Published on Web 06/24/2008

Although the field of magnetically important Cu^{II} complexes has been extensively studied, fewer Schiff base complexes containing a linear trinuclear array of copper centers have been reported. One approach for the synthesis of multinuclear complexes of copper is the introduction of tri- or tetradentate Schiff base ligands with suitable donor sets capable of holding together two or more metal ions.[12] The reactions of H_2salen or related ligands with metal ions yield complexes in which the oxygen atoms of the deprotonated Schiff base can bridge another metal ion to form multinuclear (homo- or heteronuclear) complexes.[13,14] An additional bridging anionic ligand like carboxylate is needed to provide the required rigidity and stability of the polynuclear structure.[15] Interestingly, most of the trinuclear complexes reported so far are of salpn [salpn is the dianion of *N*,*N*′-bis(salicylidene)propane-1,3-diamine] and contain the additional anion bridge. It is well-known that a carboxylate group can bridge metal ions to give rise to a wide variety of polynuclear complexes ranging from discrete entities to three-dimensional systems.[16] Carboxylate groups can adopt different kinds of bridging conformations, the most important being syn−syn, syn−anti, anti−anti, and oxo. The rich chemistry of these complexes has been applied to the investigation of magnetic exchange interactions between metal ions. The predominant magnetic interaction between metal centers in the commonly known polynuclear Cu^{II} complexes is antiferromagnetic, as observed in the antiferromagnetically coupled metal centers present in the active sites of multicopper enzymes,[17] whereas ferromagnetic interactions in linear trinuclear Cu^{II} Schiff base complexes are comparatively rare.[18,19] Magnetostructural correlations in multinuclear Cu^{II} complexes bridged by pairs of alkoxide or phenoxide groups show that the major factor controlling spin coupling (*J*) between the metal centers is the Cu−O−Cu angle (Φ) and is also simultaneously related to the bridging conformation adopted by the carboxylate group present in these polynuclear systems.[20,21]

In a continuation of our earlier studies[20] on the phenoxo-bridged multinuclear Cu^{II} Schiff base complexes, this paper contains systematic structural and magnetic studies of two new linear trimeric Cu^{II} Schiff base complexes with bridging carboxylates in a syn–syn fashion. Density functional theory (DFT) calculations and continuous-shape measurement (CShM) studies have also been performed on the trinuclear functional unit to reveal the most plausible mechanism of the antiferromagnetic interaction.

Experimental Section

Materials. All of the chemicals and solvents used for the syntheses were of high-purity analytical grade. $Cu_2(CH_3COO)_4 \cdot 2H_2O$, 2-hydroxyacetophenone, 1,3-diaminopropane, and triethylamine were purchased from Aldrich Chemical Co. Inc. and used without any further purification. Hydrated copper(II) trifluoroacetate was prepared by the treatment of basic copper(II) carbonate, $CuCO_3 \cdot Cu(OH)_2$ (AR grade, E. Merck, India), with 60% trifluoroacetic acid (AR grade, E. Merck, India), followed by slow evaporation on a steam bath. It was then filtered through a fine glass frit and stored in a $CaCl_2$ desiccator.

Physical Measurements. The Fourier transform IR (FT-IR) spectra were recorded on a Perkin Elmer Spectrum RX I FT-IR system with a KBr disk in the range 4000−200 cm^{-1}. The electronic spectra were recorded on a Perkin Elmer Lambda 40 UV/vis spectrometer using high-performance liquid chromatography grade methanol in the range 200−800 nm. Elemental analyses (C, H, and N) were carried out using a Perkin Elmer 2400 II elemental analyzer. Electron paramagnetic resonance (EPR) spectra of **1** and **2** were recorded on polycrystalline samples or in CH_3CN and *N*,*N*-dimethylformamide (DMF) solutions with an X-band Bruker EMX spectrometer at 298 and 120 K. The spectra were simulated with the computer program Bruker WinEPR SimFonia. Cryomagnetic susceptibility measurements for the two complexes were carried out on polycrystalline samples with a Quantum Design SQUID MPMS-XL susceptometer apparatus working in the range 2−300 K under a magnetic fields of approximately 500 G (2−30 K) and 1000 G (35−300 K). Diamagnetic corrections were estimated from Pascal's tables.

Syntheses of the Schiff Base Ligand and Complexes. *N*,*N*′-Bis(2-hydroxyacetophenone)propylenediimine (H_2L). The Schiff base ligand $(OH)C_6H_4(CH_3)C{=}N(CH_2)_3N{=}C(CH_3)C_6H_4$-

(12) (a) Tuna, F.; Patron, L.; Journaux, Y.; Andruh, M.; Plass, W.; Trombe, J.-C. *J. Chem. Soc., Dalton Trans.* **1999**, 539. (b) Chen, X.; Zhan, S.; Hu, C.; Meng, Q.; Liu, Y. *J. Chem. Soc., Dalton Trans.* **1997**, 245. (c) Paital, A. R.; Nanda, P. K.; Das, S.; Aromí, G.; Ray, D. *Inorg. Chem.* **2006**, *45*, 505.

(13) Carbonaro, L.; Isola, M.; La Pegna, P.; Senatore, L.; Marchetti, F. *Inorg. Chem.* **1999**, *38*, 5519.

(14) Yamaguchi, T.; Sunatsuki, Y.; Kojima, M.; Akashi, H.; Tsuchimoto, M.; Re, N.; Osa, S.; Matsumoto, N. *Chem. Commun.* **2004**, 1048.

(15) Colacio, E.; Dominguez-Vera, J. M.; Moreno, J. M.; Riuz, J.; Kivekäs, R.; Romerosa, A. *Inorg. Chim. Acta* **1993**, *212*, 115.

(16) (a) Rettig, S. J.; Thompson, R. C.; Trotter, J.; Xia, S. *Inorg. Chem.* **1999**, *38*, 1360. (b) Tangoulis, V.; Psomas, G.; Dendrinou-Samara, C.; Raptopoulou, C. P.; Terzis, A.; Kessissoglou, D. P. *Inorg. Chem.* **1996**, *35*, 7655.

(17) Solomon, E. I.; Sundaram, U. M.; Machonkin, T. E. *Chem. Rev.* **1996**, *96*, 2563.

(18) Mukhopadhyay, S.; Mandal, D.; Chatterjee, P. B.; Desplanches, C.; Sutter, J.-P.; Butcher, R. J.; Chaudhury, M. *Inorg. Chem.* **2004**, *43*, 8501.

(19) Gutierrez, L.; Alzuet, G.; Real, J. A.; Cano, J.; Borrás, J.; Castiñeiras, A. *Inorg. Chem.* **2000**, *39*, 3608.

(20) (a) Dey, S. K.; Bag, B.; Malik, K. M. A.; El Fallah, M. S.; Ribas, J.; Mitra, S. *Inorg. Chem.* **2003**, *42*, 4029. (b) Dey, S. K.; Bag, B.; Zhou, Z.; Chan, A. S. C.; Mitra, S. *Inorg. Chim. Acta* **2004**, *357*, 1991. (c) Saha, M. K.; Dey, D. K.; Samanta, B.; Edwards, A. J.; Clegg, W.; Mitra, S. *Dalton Trans.* **2003**, 488. (d) Datta, A.; Choudhury, C. R.; Talukder, P.; Mitra, S.; Dahlenburg, L.; Matsushita, T. *J. Chem. Res. (S)* **2003**, 642.

(21) (a) Orvan, P. J.; Estes, W. E.; Weller, R. R.; Hatfield, W. E. *Inorg. Chem.* **1980**, *19*, 1297. (b) Carlin, R. L.; Kopinga, K.; Kahn, O.; Verdaguer, M. *Inorg. Chem.* **1986**, *25*, 1786. (c) Dell'Amico, D. B.; Alessio, R.; Calderazzo, F.; Pina, F. D.; Englert, U.; Pampaloni, G.; Passarelli, V. *J. Chem. Soc., Dalton Trans.* **2000**, 2067. (d) Towle, D. K.; Hoffman, S. K.; Hatfield, W. E.; Singh, P.; Choudhuri, P. *Inorg. Chem.* **1988**, *27*, 94. (e) Levstein, P. R.; Calvo, R. *Inorg. Chem.* **1990**, *29*, 1581.

(22) (a) *Apex 2*, version 2.2; Bruker AXS Inc.: Madison, WI, 2006. (b) Sheldrick, G. M. *SADABS, Programs for Area Detector Adsorption Correction*; Institute for Inorganic Chemistry, University of Göttingen: Göttingen, Germany. (c) Sheldrick, G. M. *SHELXTL, Program for the Solution and Refinement of Crystal Structures*, version 5.1; Bruker AXS, Inc.: Madison, WI, 1999. (d) Spek, A. L. *PLATON, Molecular Geometry Program*; University of Utrecht: Utrecht, The Netherlands, 1999. (e) ORTEP3 for Windows: Farrugia, L. J. *J. Appl. Crystallogr.* **1997**, *30*, 565.

(23) (a) Dolaz, M.; Tümer, M.; Diğrak, M. *Transition Met. Chem.* **2004**, *29*, 528. (b) You, Z.-L.; Zhu, H.-L. *Z. Anorg. Allg. Chem.* **2004**, *630*, 2754. (c) Nakamoto, K. *Infrared and Raman Spectra of Inorganic and Coordination Compounds, Theory and Applications in Inorganic Chemistry*, 5th ed.; John Wiley and Sons, Inc.: New York, 1997. (d) Tarafder, M. T. H.; Kasbollah, A.; Crouse, K. A.; Ali, A. M.; Yamin, B. M.; Fun, H.-K. *Polyhedron* **2001**, *20*, 236.

Table 1. Crystal Data, Data Collection, and Refinement Parameters of **1** and **2**

	1	**2**
formula	$C_{42}H_{46}Cu_3N_4O_8$	$C_{42}H_{40}Cu_3F_6N_4O_8$
fw (g mol^{-1})	925.48	1033.43
cryst size (mm^3)	0.35 × 0.20 × 0.12	0.30 × 0.25 × 0.10
cryst syst	monoclinic	monoclinic
space group	$P2_1/c$ (No. 14)	$P2_1/n$ (No. 14)
a (Å)	10.6100(6)	12.4695(12)
b (Å)	19.3364(12)	10.6836(9)
c (Å)	9.9334(5)	14.9603(13)
β (deg)	116.350(2)	97.393(5)
V (Å^3)	1826.19(18)	1976.4(3)
Z	2	2
ρ_{calcd} (g cm^{-3})	1.683	1.737
$\lambda_{Mo\ K\alpha}$ (Å)	0.71073	0.71073
T (K)	100	100
μ (mm^{-1})	1.795	1.689
θ_{min}, θ_{max} (deg)	2.1, 30.2	3.0, 26.0
total data, unique data	13 645, 4715	75 072, 3888
obsd data [$I > 2\sigma(I)$]	3530	2561
R^a	0.0367	0.0422
$R_w{}^b$	0.0804	0.1020
S	1.02	1.01
$\Delta\rho_{max}$ (e Å^{-3})	0.53	0.47
$\Delta\rho_{min}$ (e Å^{-3})	−0.43	−0.69

^{a} $R = \sum||F_o| - |F_c||/\sum|F_o|$. ^{b} $R^w = \{\sum[w(|F_o| - |F_c|)^2]/\sum[w|F_o|^2]\}^{1/2}$.

(OH), or H_2L, was prepared by the reflux condensation of 2-hydroxyacetophenone (0.272 g, 2 mmol) and 1,3-diaminopropane (0.074 g, 1 mmol) in 20 mL of methanol for 1 h. The resulting solution yielded shiny yellow crystals of the ligand upon slow evaporation. They were dried and stored in vacuo over $CaCl_2$ for subsequent use. Yield: 0.263 g (85%). Anal. Calcd for $C_{19}H_{22}N_2O_2$ (M = 310.39 g mol^{-1}): C, 73.52; H, 7.14; N, 9.03. Found: C, 73.41; H, 7.11; N, 9.01. Characteristic IR absorptions (KBr, cm^{-1}): 1623 s ($\nu_{C=N}$). UV/vis (λ, nm): 241, 371.

[Cu$_3$(L)$_2$(CH$_3$COO)$_2$] (1). The appropriate quantity of solid Schiff base ligand H_2L (0.621 g, 2 mmol) was dissolved in 20 mL of methanol. A solution of $Cu_2(CH_3COO)_4 \cdot 2H_2O$ (0.653 g, 3 mmol) in 10 mL of methanol was added to this solution. The mixture was refluxed for 45 min at 65 °C. The resulting deep-green solution was then filtered and kept undisturbed. After 2 days, green block-shaped X-ray diffraction quality single crystals were separated out from the filtrate. Yield: 0.821 g (89%). Anal. Calcd for $C_{42}H_{46}Cu_3N_4O_8$ (M = 925.47 g mol^{-1}): C, 54.51; H, 5.01; N, 6.05. Found: C, 54.48; H, 4.99; N, 6.01.

[Cu$_3$(L)$_2$(CF$_3$COO)$_2$] (2). The complex was prepared following the same procedure as that described above for **1** except that copper(II) trifluoroacetate and the Schiff base were taken in the proportion of 0.977 g, 3 mmol, and 0.621 g, 2 mmol, respectively. Deep-green prismatic single crystals were obtained from the reaction mixture after 3 days. Yield: 0.910 g (90%). Anal. Calcd for $C_{40}H_{46}Cu_3F_6N_4O_8$ (M = 1015.44 g mol^{-1}): C, 47.31; H, 4.57; N, 5.52. Found: C, 47.29; H, 4.55; N, 5.49.

Crystallographic Data Collection and Refinement. Intensity data were collected on single crystals of **1** and **2** at 100 K on a Bruker X8 Apex 2 CCD diffractometer equipped with a graphite monochromator and Mo Kα radiation (λ = 0.71073 Å) using the Bruker Apex2 software.[22a] Multiscan absorption correction was applied using *SADABS*.[22b] All non-hydrogen atoms were refined anisotropically. Hydrogen atoms of the aromatic rings and the methyl, methylene, and imine (CH=N) groups were constrained to ideal geometry and treated as riding on the bound atom. All of the crystallographic computations were carried out using *SHELXTL*,[22c] *PLATON 99*,[22d] and *ORTEP*[22e] programs. Further crystallographic data are summarized in Table 1.

Results and Discussion

FT-IR Spectroscopy. A strong sharp absorption band around 1623 cm^{-1} in the spectrum of the Schiff base ligand may be assigned for the imine stretching frequency. This band is shifted to the lower wave numbers upon complexation with the metal by 20−40 cm^{-1}, which can be attributed to the coordination of the nitrogen atom of the imine group to the metal ions.[11,23a] The phenolic ν_{Ar-O} in the free ligand exhibits a strong band at 1201 cm^{-1}. However, in the complexes, this band also shifts to the lower frequency region at about 1181−1186 cm^{-1}, providing evidence for coordination to the metal ions through the deprotonated phenolic oxygen atoms.[23b] Sharp bands appearing at nearly 420 and 375 cm^{-1} correspond to the Cu−N and Cu−O stretching frequencies, respectively, in the complexes. In **1**, vibrationally active acetate ligands display asymmetric and symmetric stretching vibrations at 1564 and 1413 cm^{-1}, respectively. Moreover, complex **2** exhibits the typical trifluoroacetate vibrations $\nu_{asym}(COO^-)$ at 1600 cm^{-1} and $\nu_{sym}(COO^-)$ at 1450 cm^{-1}. The difference between $\nu_{asym}(COO^-)$ and $\nu_{sym}(COO^-)$, $\Delta\nu$, in the complexes is about 150 cm^{-1}, which is smaller than 164 cm^{-1} observed in free acetate and trifluoroacetate ion, indicating the presence of a deprotonated carboxylate group coordinated to the metal centers in a bridging bidentate fashion.[23c,d]

Electronic Spectra. In the complexes, the bands in the 465−335 nm range may be assigned for the n → π^* transition of the imine group[24] and the bands at higher energies (300−210 nm) are associated with the aromatic π → π^* intraligand charge-transfer transitions. The spectra of the complexes also show intense bands at 305−375 nm, attributable to ligand-to-metal charge-transfer transitions from the coordinated unsaturated ligand to the metal ion.[25] A broad band in the range 620−650 nm can be correlated to the d−d transition, which is typical for a Cu^{II} Schiff base complex.[26]

Description of the Crystal Structures. A perspective ORTEP view with the atom-labeling scheme of the trimeric asymmetric unit of **1** is presented in Figure 1. The molecular structure of **2** exhibits very similar features and is shown in Figure 2. Selected bond lengths and angles for complexes **1** and **2** are given in Table 2. Both of the centrosymmetric complexes show a linear trinuclear array of three Cu^{II} ions, where two μ-phenolato oxygen atoms of the deprotonated Schiff base ligand L^{2-} and one bidentate bridging (μ^2−η^1:η^1) CX_3COO^- anion (where X = H and F for **1** and **2**, respectively) bridge each terminal copper atom to the central copper atom. Both of the carboxylates bridge the terminal Cu1 and central Cu2 centers in a syn−syn fashion but are mutually trans to each other, owing to inversion symmetry. The IR spectra of the complexes provide useful information

(24) Golcu, A.; Tümer, M.; Demirelli, H.; Wheatley, R. A. *Inorg. Chim. Acta* **2005**, *358*, 1785.
(25) Tümer, M. *Synth. React. Inorg. Met.−Org. Chem.* **2000**, *30*, 1139.
(26) Dieng, M.; Thiam, I.; Gaye, M.; Sall, A. S.; Barry, A. H. *Acta Chim. Slov.* **2006**, *53*, 417.
(27) (a) *Comprehensive Coordination Chemistry*; Hathaway, B. J., Wilkinson, G., Gillard, R. D., McCleverty, J. A., Eds.; Pergamon: New York, 1987; Vol. *5*, p 607. (b) Addison, A. W.; Rao, T. N.; Reedijk, J.; Van Rijn, J.; Verschoor, G. C. *J. Chem. Soc., Dalton Trans.* **1984**, 1349.

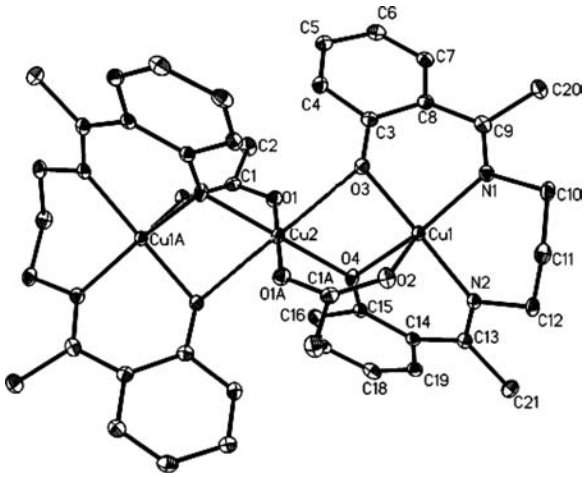

Figure 1. ORTEP view of **1** with an atom-labeling scheme. Ellipsoids are at the 50% probability level. Hydrogen atoms have been omitted for clarity (symmetry code: A = $-x$, $-y$, $-z$).

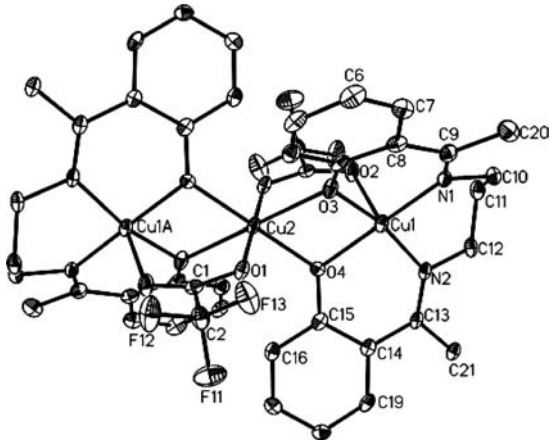

Figure 2. ORTEP view of **2** with an atom-labeling scheme. Ellipsoids are at the 50% probability level. Hydrogen atoms have been omitted for clarity (symmetry code: A = $-x$, $-y$, $-z$).

Table 2. Selected Bond Lengths (Å) and Bond Angles (deg) for **1** and **2**

bond length	**1**	**2**	bond angle	**1**	**2**
Cu1−N1	1.980(2)	1.995(3)	N1−Cu1−N2	92.86(9)	97.70(13)
Cu1−N2	1.984(2)	1.990(3)	N1−Cu1−O3	88.23(9)	89.94(12)
Cu1−O3	1.9267(18)	1.903(2)	N2−Cu1−O4	89.45(8)	88.24(12)
Cu1−O4	1.9810(2)	1.984(3)	O3−Cu1−O4	87.57(8)	82.98(10)
Cu1−O2	2.2305(18)	2.312(3)	N1−Cu1−O4	155.80(8)	169.43(12)
Cu2−O1	1.9317(18)	1.981(2)	N2−Cu1−O3	175.01(8)	168.61(13)
Cu2−O4	2.0002(18)	1.987(2)	O2−Cu1−O3	91.90(7)	90.20(11)
Cu2−O3	2.454(2)	2.331(3)	O2−Cu1−O4	86.15(7)	85.90(10)
C1−O1	1.277(3)	1.269(5)	N1−Cu1−O2	117.80(8)	102.02(12)
C1−O2A[a]	1.247(3)	1.222(5)	N2−Cu1−O2	91.89(7)	96.41(12)
N1−C9	1.292(3)	1.312(5)	O1−Cu2−O4	91.02(8)	91.46(10)
			O1−Cu2−O3	87.80(7)	84.36(9)
			O3−Cu2−O4	73.98(7)	72.77(9)

[a] Symmetry code: A = $-x$, $-y$, $-z$.

about the bridging mode of the bidentate carboxylate. The separation value between $\nu_{asym}(COO^-)$ and $\nu_{sym}(COO^-)$, $\Delta\nu \sim 150$ cm^{-1}, is a clear indication of the bidentate syn−syn bridging mode of the carboxylate.[20]

The coordination geometry of the central Cu^{II} ion has typical Jahn−Teller distortion, as is expected for a Cu^{II} d^9 system, from ideal octahedral geometry. The equatorial plane of the central Cu2 is constructed by two bridging phenoxo oxygen atoms (O4 and its symmetry-related counterpart O4A) from two Schiff base ligands and two oxygen atoms (O1 and O1A) from the two bridging carboxylates, while the apical positions of the octahedron are occupied by the two bridging phenoxo oxygen atoms O3 and O3A. Because the central Cu2 atom is located on an inversion center, all three trans angles are 180°. In the coordination sphere of Cu2 in complex **1**, the equatorial Cu2−O(phenoxo) and Cu2−O(acetate) bond lengths are distinctly shorter than the axial Cu2−O(phenoxo) distances (Table 2). Similarly, in complex **2**, the central Cu2 ion forms four short bonds in the equatorial plane. Again the longest Cu−O bond is to the bridging phenoxo oxygen along the axial direction, but this is significantly shorter than the corresponding bond in complex **1** (Cu2−O3 = 2.454(2) and 2.331(3) Å for complexes **1** and **2**, respectively).

In both complexes, two terminal copper atoms are pentacoordinated, bearing identical environments, owing to the crystallographic inversion symmetry. The coordination number 5 for Cu^{II} is very common, where it may possess either square-pyramidal (SP) or trigonal-bipyramidal (TBP) geometry. For a pentacoordinated metal center, the distortion of structure from TBP to SP can be evaluated by the Addison distortion index, τ, defined as the ratio of the mean in-plane Cu−L bond distance to the out-of-plane Cu−L bond distance,[27a] $\tau = [|\theta - \Phi|/60]$, where θ and Φ are the two largest coordination angles and $\tau = 0$ for perfect SP and 1 for ideal TBP.[27b] In complexes **1** and **2**, the calculated τ values are 0.32 and 0.01, respectively, as is found for the terminal copper atoms. This clearly suggests a distorted SP geometry for the terminal copper atoms in complex **1**, while it is a perfect SP one in the case of complex **2**. The equatorial plane of each of the two equivalent terminal copper atoms is formed by the two imine nitrogen atoms (N1 and N2) and two phenolic oxygen atoms (O3 and O4). The apical position is occupied by an oxygen atom from the bridging carboxylate group (O2). Cu1 is displaced from the mean equatorial plane constructed by two imine nitrogen atoms and two phenolic oxygen atoms of the Schiff base ligand by 0.244(3) and 0.139(2) Å in complexes **1** and **2**, respectively, toward the axial oxygen. The two six-membered $CuONC_3$ chelate rings are found to possess half-chair conformations, while the CuN_2C_3 chelate ring has a pronounced boat conformation. In the first complex, the Cu1−imine nitrogen and Cu1−phenolic oxygen bond distances are in the ranges observed for similar systems.[28,29] Similarly, in the later one, Cu−O equatorial distances around the terminal Cu1 ions [1.903(2)−1.984(3) Å] are shorter than the axial Cu1−O2 bond distance of 2.312(3) Å. The Cu1−N distances [1.990(3) and 1.995(3) Å] are also comparable to those observed in similar systems.[30] The bridging carboxylate group coordinates to the central Cu2 along the equatorial plane, while it

(28) (a) Chakraborty, J.; Samanta, B.; Pilet, G.; Mitra, S. *Inorg. Chem. Commun.* **2007**, *10*, 40. (b) Majumder, A.; Rosair, G.; Mallick, A.; Chattopadhyay, N.; Mitra, S. *Polyhedron* **2006**, *25*, 1753.
(29) Blackman, A. G. *Polyhedron* **2005**, *24*, 1.
(30) Mukherjee, A.; Saha, M. K.; Nethaji, M.; Chakravarty, A. R. *Polyhedron* **2004**, *23*, 2177.

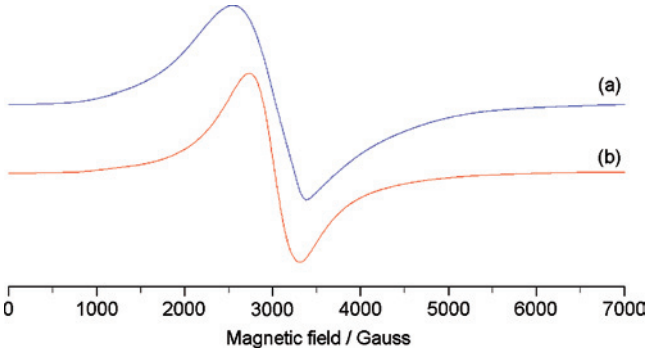

Figure 3. X-band EPR spectra recorded on the polycrystalline sample of **1**: (a) 298 K and (b) 120 K.

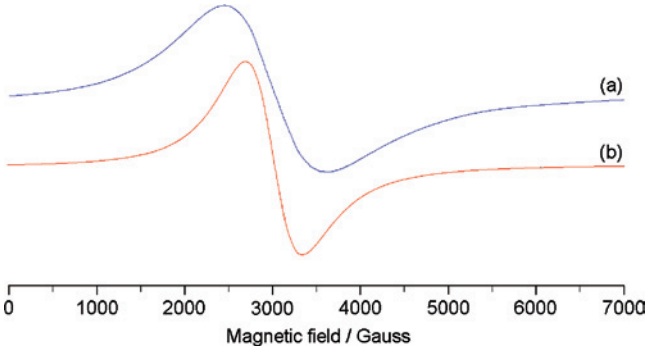

Figure 4. X-band EPR spectra recorded on the polycrystalline sample of **2**: (a) 298 K and (b) 120 K.

occupies the axial site of the terminal Cu1 atom. Both of these equatorial and axial Cu−O(acetate) distances are significantly shorter in the case of complex **1**, as compared to similar bonds present in complex **2**. Considering that the only difference between the two complexes is the $-CH_3$ group in the first one and the $-CF_3$ group in the later, the greater electron-withdrawing effect of the $-CF_3$ group appears to be responsible for the elongation of the equatorial Cu2−O1 and axial Cu1−O2 bonds in complex **2**. In complex **1**, H11a of the saturated portion of the Schiff base is 2.49 Å from O2 (acetate) and is the closest C−H−O contact. The same feature is found in complex **2** also where O2 (trifluoroacetate) is 2.34 Å away from H11b.

EPR Measurements. The trimeric polycrystalline solid complexes exhibit a single isotropic feature with g values of 2.218 and 2.210 at 298 and 120 K, respectively, for complex **1** (Figure 3). The corresponding values are 2.222 and 2.231 for complex **2** (Figure 4).

Such isotropic absorptions are usually the results of intramolecular spin exchange, probably due to the strong spin coupling among the paramagnetic ions, thereby broadening the lines. Measurement at temperatures lower than 298 K shows the reduction of the line width (cf. parts a and b of Figure 3 and parts a and b of Figure 4).

The EPR spectrum of **1** dissolved in CH_3CN and DMF at 120 K shows the characteristic resonances of monomeric Cu^{II} species and an axial symmetry with a well-resolved hyperfine (hf) structure (Figure 5). The signals attributable to the solvated Cu^{II} ions are found to be absent, indicating the possible dissociation of the polymeric entity to yield a 1:1

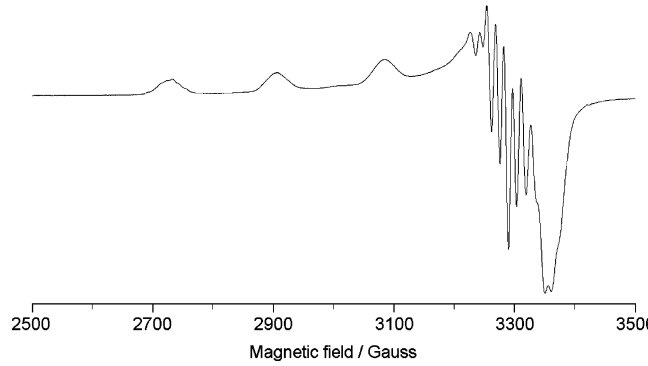

Figure 5. X-band EPR spectrum of **1** dissolved in CH_3CN or DMF at 120 K.

species with a square-planar geometry. Such a possibility has been reported for other trimeric Cu^{II} complexes.[31] The spectral parameters $g_{||} = 2.242$ and $A_{||} = 188.2 \times 10^{-4}$ cm^{-1} in CH_3CN and $g_{||} = 2.240$ and $A_{||} = 192.6 \times 10^{-4}$ cm^{-1} in DMF show good agreement with those reported for square-planar Cu^{II} complexes formed by salicylaldiimine or related salen derivatives.[32–35]

A superhyperfine (shf) structure is also visible in the first parallel absorption and in the perpendicular region of the spectrum (Figure 5), which may be attributed to the interaction of the unpaired electron on the Cu^{II} ion with the two ^{14}N equivalent nuclei ($I = 1$). In similar cases, a higher number of lines than the five expected has been explained as a further shf coupling with two distant imine ^{1}H nuclei ($I = {}^1/_2$).[32,36] The absence of these protons in **1** and **2** suggests that another factor such as the presence of other isotopes of copper (^{63}Cu and ^{65}Cu) could be responsible for this effect, enhancing the number of absorptions. The mean value of 15×10^{-4} cm^{-1} for A_N is in good agreement with that reported in the literature.[35] After dissolution in DMF, **2** shows a spectrum comparable to that of **1** and similar to those of other Cu^{II} salen complexes: EPR parameters are $g_{||} = 2.240$ and $A_{||} = 188.0 \times 10^{-4}$ cm^{-1}. On the other hand, complex **2** is poorly soluble in CH_3CN and is characterized by an unresolved spectrum similar to that observed in the solid state.

Cryomagnetic Susceptibility Studies. The global feature of the $\chi_M T$ vs T curves in **1** and **2** is a characteristic of antiferromagnetic interaction of linear trinuclear Cu^{II} with very slight differences. The value of $\chi_M T$ at 300 K is 1.248 cm^3 K mol^{-1} for **1** and 1.208 cm^3 K mol^{-1} for **2** (Figure 6), which is close to that expected for three uncoupled Cu^{II} ions (1.240 cm^3 K mol^{-1} per three Cu^{II} with $g = 2.1$). This value decreases gradually (more quickly in the case of **2** than **1**), reaching 0.453 cm^3 K mol^{-1} at 9.2 K for **1** and 0.461 cm^3 K

(31) Strinna Erre, L.; Garribba, E.; Micera, G.; Pusino, A.; Sanna, D. *Inorg. Chim. Acta* **1997**, *255*, 215.
(32) Maki, A. H.; McGarvey, B. R. *J. Chem. Phys.* **1958**, *29*, 35.
(33) Hasty, E. F.; Colburn, T. J.; Hendrikson, D. N. *Inorg. Chem.* **1973**, *12*, 2414.
(34) Charles, E. H.; Chia, L. M. L.; Rothery, J.; Watson, E. L.; McInnes, E. J. L.; Farley, R. D.; Bridgeman, A. J.; Mabbs, F. E.; Rowlands, C. C.; Halcrow, M. A. *J. Chem. Soc., Dalton Trans.* **1999**, 2087.
(35) Klement, R.; Stock, F.; Elias, H.; Paulus, H.; Pelikán, P.; Valko, M.; Mazúr, M. *Polyhedron* **1999**, *18*, 3617.
(36) Kita, S.; Hashimoto, M.; Iwaizumi, M. *Inorg. Chem.* **1979**, *18*, 3432.

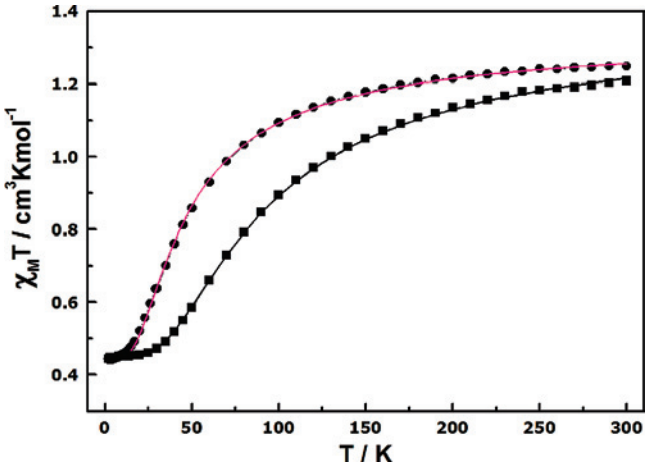

Figure 6. Plot of observed $\chi_M T$ vs T: (●) for complex **1** and (■) for complex **2** (the molar value refers to three copper atoms). Solid lines correspond to the best fit.

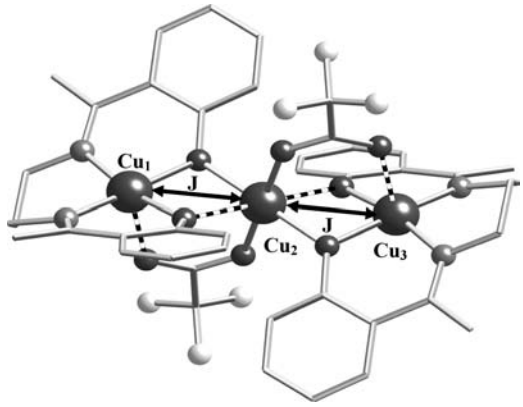

Figure 7. Structural representation with exchange coupling constants of complex **2**. Multiband cylinder bonds indicate the longer Cu···O distance (~2.3 Å).

mol^{-1} at ~25 K for **2**. In the two cases, a plateau is observed between these temperatures and 2 K.

The analysis of the experimental susceptibility data has been performed[37] by the use of eq 1, considering two equal J exchange couplings as indicated in Figure 7.

$$\chi_M = \frac{Ng^2\beta^2}{4kT}\left[\frac{1+e^{J/kT}+10e^{3J/2kT}}{1+e^{J/kT}+2e^{3J/2kT}}(1-\rho)+\rho\right] \qquad (1)$$

The energy values can be obtained using the Kambe method[37] from the Hamiltonian:

$$H = -J(S_1S_2 + S_2S_3)$$

In eq 1, we have taken into account a proportion of a monomeric impurity (ρ), for which the susceptibility is assumed to follow the Curie law $\chi = (Ng^2\beta^2/kT)$. The parameters N, g, β, and k in eq 1 have their usual meanings, where J = doublet−quartet splitting. Least-squares fitting of all of the experimental data leads to the following parameters: $J = -36.5 \pm 0.3$ cm^{-1}, $\rho = 0.013$, and $g = 2.19$ for complex **1** and $J = -72.3 \pm 0.5$ cm^{-1}, $\rho = 0.021$, and $g = 2.20$ for complex **2**. The agreement $R = \sum_i(\chi T_{i,\text{calcd}} - \chi T_{i,\text{exp}})^2/(\chi T_{i,\text{exp}})^2$ in both cases is less than 10^{-5}.

(37) Kambe, K. *J. Phys. Soc. Jpn.* **1950**, *5*, 48.

DFT Calculations (B3LYP Functional) and CShM Studies. In order to examine the above results and understand the mechanism of magnetic coupling, DFT calculations have been performed using the atomic coordinates of the whole trinuclear functional unit of the complexes, as revealed from their single-crystal X-ray structures. The calculated J values (described in the Computational Methodology section) are found to be −10 and −26 cm^{-1} for **1** and **2**, respectively. These values though appear to be less than the experimentally fitted ones but are quite able to give a good qualitative agreement: (i) the sign and the moderate antiferromagnetic interaction; (ii) the relatively low exchange coupling in the case of complex **1** compared to that of complex **2**. From the DFT calculations, the distortion in the metal ion geometry and the extent of orbital mixing are reflected in the difference of J values between the two complexes.

It is well-known that the magnetic behavior of divalent copper complexes bridged equatorially by a pair of phenoxide[38] oxygen atoms is highly dependent on the Cu−O−Cu bridge angle. Additionally, the Cu−O(bridge) distance, the Cu···Cu separation, the geometries around the copper center, and the bridging oxygen atom can also influence the coupling even though in smaller measure. In our cases too, the exchange coupling (J) can be explained in terms of the geometrical distortions that affect the copper coordination spheres, the geometry of the bridges, and the planarity of the bridge core. In the case of complexes **1** and **2**, the equatorial planes containing the $d_{x^2-y^2}$ orbitals are rotated, leaving a relatively perpendicular orientation. This situation is comparable to dinuclear Cu^{II} complexes with double phenoxo bridges, where the overlap between the Cu $d_{x^2-y^2}$ orbital and the p orbital of the oxygen atom of the phenoxo group decreases if one of the equatorial planes that contain the $d_{x^2-y^2}$ orbital rotates versus the other one along an axis other than the bonding axis. This also causes one of the two Cu−O(phenoxo) distances to become large, as observed in the case of complexes **1** and **2** (Figure 7). For complexes **1** and **2**, the relatively perpendicular orientation of the $d_{x^2-y^2}$ orbitals reduces the extent of overlap between the magnetic orbitals, thereby decreasing the antiferromagnetism, although there is sufficient overlap of each $d_{x^2-y^2}$ orbital with the phenoxide oxygen p orbital to generate negative J values of intermediate magnitude[39] (Figure 8). It is necessary to indicate here that the difference found in the J values between

(38) (a) Gupta, R.; Mukherjee, S.; Mukherjee, R. *J. Chem. Soc., Dalton Trans.* **1999**, 4025. (b) Adams, H.; Bailey, N. A.; Campbell, I. K.; Fenton, D. E.; He, Q.-Y. *J. Chem. Soc., Dalton Trans.* **1996**, 2233. (c) Block, D.; Blake, A. J.; Dancey, K. P.; Harrison, A.; McPatlin, M.; Parsons, S.; Tasker, P. A.; Whitlaker, G.; Schröder, M. *J. Chem. Soc., Dalton Trans.* **1998**, 3953. (d) Sunatsuki, Y.; Nakamura, M.; Matsumoto, N.; Kai, F. *Bull. Chem. Soc. Jpn.* **1997**, *70*, 1851. (e) Vaidyatham, M.; Viswanathan, R.; Palaniandavar, M.; Balasubramanian, T.; Prabhaharan, P.; Muthiah, T. P. *Inorg. Chem.* **1998**, *37*, 6418. (f) Sangeetha, N. R.; Baradi, K.; Gupta, R.; Pal, C. K.; Manivannan, V.; Pal, S. *Polyhedron* **1999**, *18*, 1425. (g) Galy, J.; Jaud, J.; Kahn, O.; Tola, P. *Inorg. Chim. Acta* **1979**, *36*, 229. (h) Tandon, S. S.; Thompson, L. K.; Bridson, J. N. *Inorg. Chem.* **1993**, *32*, 32. (i) Dutta, S. K.; Florke, U.; Mohanta, S.; Nag, K. *Inorg. Chem.* **1998**, *37*, 5029. (j) Thompson, L. K.; Mandal, S. K.; Tandon, S. S.; Bridson, J. N.; Park, M. K. *Inorg. Chem.* **1996**, *35*, 3117. (k) Xie, Y.; Jiang, H.; Chan, A. S. C.; Liu, Q.; Xu, X.; Du, C.; Zhu, Y. *Inorg. Chim. Acta* **2002**, *333*, 138.

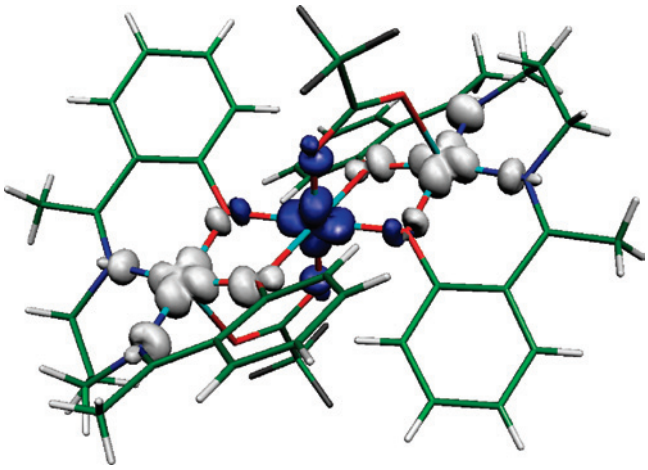

Figure 8. Spin-density distribution for complex **2** corresponding to the $S = {}^1/_2$ ground-state single-determinant B3LYP solution. Positive and negative values are represented as white and dark surfaces, respectively. In some bridging oxygen atoms, there are two lobes with spin densities of different sign that appear because of the presence of neighboring Cu^{II} cations with opposite spin densities; probably this spin density is an artifact due to the single-determinant wave function considered.

the two complexes is not due to the bridge angles, but it is the distortion in the geometry of the terminal Cu^{II} ions that is responsible for that fact because these Cu−O$_{Ph}$−Cu angles are more or less similar in both complexes: 103.11° and 89.93° for **1** and 103.87° and 94.67° for **2**. In complexes **1** and **2**, the calculated τ values are 0.32 and 0.01, respectively, suggesting a distorted SP geometry for the terminal copper atoms in **1**, while it is a perfectly SP in the case of **2**. This implies that in complex **2** the $d_{x^2-y^2}$ magnetic orbital is majorly located in the basal plane in order to ensure a more efficient overlap, resulting in a relatively larger J value, whereas in **1**, a small distortion of the SP geometry toward the TBP geometry allows the magnetic orbital to acquire some d_{z^2} character, causing a diminution of the magnetic coupling. This explains well the relatively lower value of the experimentally found J in **1** compared to that in **2**, a fact that has also invariably been corroborated by the theoretically calculated J value.

To give a deep insight, we have further studied the geometry of the terminal copper atoms of the trinuclear system using the CShM studies proposed by Avnir and Alvarez and co-workers.[40,41] According to this theory, if a structure Q is fully coincident in shape with reference polyhedron P, then $S_Q(P) = 0$ [the expression of $S_Q(P)$ is given under the Computational Methodology section]; deviation of the value from 0 measures the departure from the ideal shape of the P polyhedron.

To compare the measures obtained for SP and the distortion to TBP, we have made a shape map (Figure 9a). This plot also represents the minimal distortion interconversion path between these two reference polyhedra considered. We may also consider the vacant octahedron (VOC) having

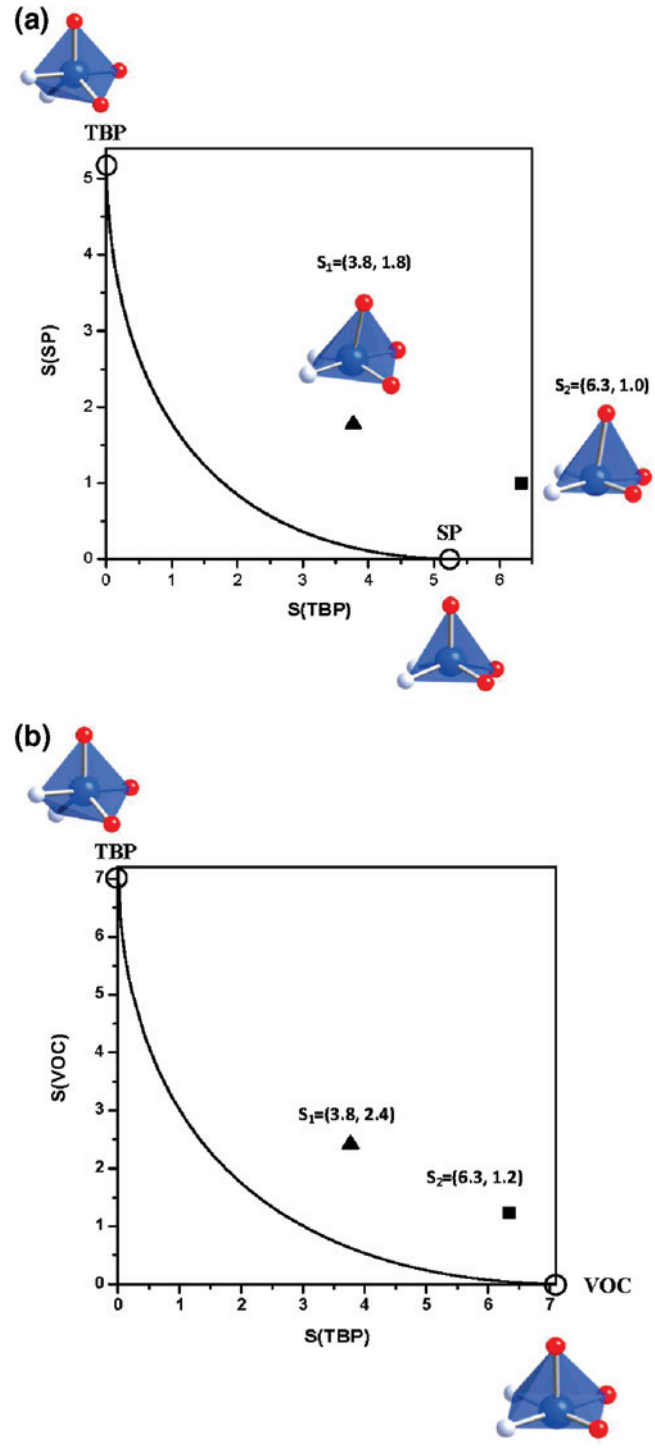

Figure 9. Minimal distortion path between (a) TBP and SP and (b) TBP and VOC. The open circles indicate the positions of two ideal shapes. The solid points indicate the positions of **1** and **2**, which are identified with the shape measures S_1 and S_2, respectively.

angles of 90° as an ideal shape. Therefore, the shape map of the minimal distortion interconversion path TBP/VOC is also represented in Figure 9b. The CShM values obtained in each case are listed in Table 3. The lowest CShM values, S(SP) = 1.8 and S(SP) = 1.0 for **1** and **2**, respectively, relative to the reference polyhedron suggest that the best structure to describe the geometry of the terminal copper atoms is SP instead of the VOC or the TBP. The results indicate that **1** and **2** are deviated more than 25% from the

(39) Choudhury, C. R.; Dey, S. K.; Karmakar, R.; Wu, C. D.; Lu, C. Z.; El Fallah, M. S.; Mitra, S. *New J. Chem.* **2003**, *27*, 1360.
(40) Zabrodsky, H.; Peleg, S.; Avnir, D. *J. Am. Chem. Soc.* **1992**, *114*, 7843.
(41) Alvarez, S.; Avnir, D.; Llunell, M.; Pinsky, M. *New J. Chem.* **2002**, *26*, 996.

Table 3. CShM for **1** and **2** Considering Three Reference Geometries (VOC, TBP, and SP)

	S(VOC)	*S*(TBP)	*S*(SP)
1	2.4	3.8	1.8
2	1.2	6.3	1.0

Scheme 1. Scheme Showing the Conversion of the Orbital Geometries of the Terminal Cu^{II} Ions

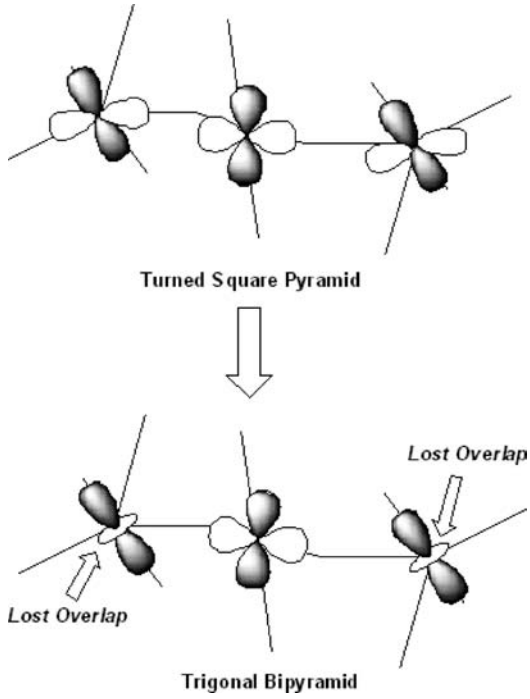

minimal interconversion path. In the case of **1**, it is clear that the geometry of the copper center is more distorted from SP than that in **2**. Consequently, the relatively weak antiferromagnetic interaction can be ascribed to the unfavorable overlaps of the magnetic orbitals for the distorted SP terminal Cu^{II} ions in **1**, compared to that of **2**. In this distortion, the contribution of the $d_{x^2-y^2}$ orbital diminishes mainly through the pathway described in Scheme 1, and the d_{z^2} orbital contribution grows in the perpendicular direction, reducing the net orbital overlap and therefore the antiferromagnetic interaction.

Computational Methodology

DFT Calculations. The exchange coupling constants in the reported linear trinuclear Cu^{II} complexes have been calculated using the following computational methodology, described previously in the literature.[42–45] Using a phenomenological Heisenberg Hamiltonian $H = -\sum J_i S_j S_k$ (where *i* labels the different kinds of coupling constants, while *j* and *k* refer to the different paramagnetic centers) to describe the exchange coupling between each pair of transition-metal ions present in the polynuclear complex, the full Hamiltonian matrix for the entire system can be constructed.

To calculate the exchange coupling constants for any polynuclear complex with *n* different exchange constants, at least the energy of $n + 1$ spin configurations must be calculated. In the case of the studied trinuclear complexes, the exchange coupling value *J* was obtained by taking into account the energy of two different spin distributions: HS (high spin) with $S = {}^3/_2$ and LS (low spin) with $S = {}^1/_2$.

The following equation has been employed to calculate the exchange coupling constant,

$$E_{HS} - E_{LS} = -2J \qquad (2)$$

The hybrid B3LYP functional[46] has been used in all calculations as implemented in *Gaussian 03*,[47] mixing the exact Hartree−Fock-type exchange with Becke's expression for the exchange functional[48] and that proposed by Lee−Yang−Parr for the correlation contribution.[49] Such an exchange functional provides calculated *J* values usually in qualitative, sometimes almost quantitative, agreement with the experimental values.[42,50,51] The use of the nonprojected energy of the broken-symmetry solution as the energy of the LS state within the DFT framework provides more or less satisfactory results because it avoids the cancellation of the nondynamic correlation effects.[52] Basis sets proposed by Schaefer et al. have been employed throughout: triple-ζ quality and two p-type polarization functions for the copper atoms[53] and double-ζ for the main-group elements.[54] The guess functions were generated with *Jaguar 6.0*.[55] All of the energy calculations were performed including 10^{-8} density-based convergence criterion.

CShM. These measures provide a method of quantitative evaluation of the shape of a given structure, to estimate the degree of distortion of a particular coordination polyhedron from a chosen ideal polyhedron. The calculation of CShM of the coordination sphere of a given atom (polyhedron Q),

(42) Ruiz, E.; Alemany, P.; Alvarez, S.; Cano, J. *J. Am. Chem. Soc.* **1997**, *119*, 1297.
(43) Ruiz, E.; Rodríguez-Fortea, A.; Cano, J.; Alvarez, S.; Alemany, P. *J. Comput. Chem.* **2003**, *24*, 982.
(44) Ruiz, E.; Cano, J.; Alvarez, S.; Alemany, P. *J. Comput. Chem.* **1999**, *20*, 1391.
(45) Ruiz, E. *Struct. Bonding* **2004**, *113*, 71.
(46) Becke, A. D. *J. Chem. Phys.* **1993**, *98*, 5648.
(47) Frisch, M. J.; Trucks, G. W.; Schlegel, H. B.; Scuseria, G. E.; Robb, M. A.; Cheeseman, J. R.; Montgomery, J. A.; Vreven, T.; Kudin, K. N.; Burant, J. C.; Millam, J. M.; Iyengar, S. S.; Tomasi, J.; Barone, V.; Mennucci, B.; Cossi, M.; Scalmani, G.; Rega, N.; Petersson, G. A.; Nakatsuji, H.; Hada, M.; Ehara, M.; Toyota, K.; Fukuda, R.; Hasegawa, J.; Ishida, H.; Nakajima, T.; Honda, Y.; Kitao, O.; Nakai, H.; Klene, M.; Li, X.; Knox, J. E.; Hratchian, H. P.; Cross, J. B.; Adamo, C.; Jaramillo, J.; Gomperts, R.; Stratmann, R. E.; Yazyev, O.; Austin, A. J.; Cammi, R.; Pomelli, C.; Ochterski, J.; Ayala, P. Y.; Morokuma, K.; Voth, G. A.; Salvador, P.; Dannenberg, J. J.; Zakrzewski, V. G.; Dapprich, S.; Daniels, A. D.; Strain, M. C.; Farkas, O.; Malick, D. K.; Rabuck, A. D.; Raghavachari, K.; Foresman, J. B.; Ortiz, J. V.; Cui, Q.; Baboul, A. G.; Clifford, S.; Cioslowski, J.; Stefanov, B. B.; Liu, G.; Liashenko, A.; Piskorz, P.; Komaromi, I.; Martin, R. L.; Fox, D. J.; Keith, T.; Al-Laham, M. A.; Peng, C. Y.; Nanayakkara, A.; Challacombe, M.; Gill, P. M. W.; Johnson, B.; Chen, W.; Wong, M. W.; Gonzalez, C.; Pople, J. A. *Gaussian 03*, revision B.4; Gaussian Inc.: Pittsburgh, PA, 2003.
(48) Becke, A. D. *Phys. Rev. A* **1988**, *38*, 3098.
(49) Lee, C.; Yang, W.; Parr, R. G. *Phys. Rev. B* **1988**, *37*, 785.
(50) Ruiz, E.; Cano, J.; Alvarez, S.; Alemany, P. *J. Am. Chem. Soc.* **1998**, *120*, 11122.
(51) Ruiz, E.; Alvarez, S.; Rodríguez-Fortea, A.; Alemany, P.; Pouillon, Y.; Massobrio, C. *Electronic Structure and Magnetic Behavior in Polynuclear Transition-Metal Compounds*; Miller, J. S., Drillon, M., Eds.; Wiley-VCH: Weinheim, Germany, 2001.
(52) Ruiz, E.; Alvarez, S.; Cano, J.; Polo, V. *J. Chem. Phys.* **2005**, *123*, 164110.
(53) Schaefer, A.; Huber, C.; Ahlrichs, R. *J. Chem. Phys.* **1994**, *100*, 5829.
(54) Schaefer, A.; Horn, H.; Ahlrichs, R. *J. Chem. Phys.* **1992**, *97*, 2571.
(55) *Jaguar 6.0*; Schrodinger Inc.: Portland, OR, 2005.

Scheme 2. Coordination Sphere of a Given Atom (Polyhedron Q), Relative to an Ideal Polyhedron P

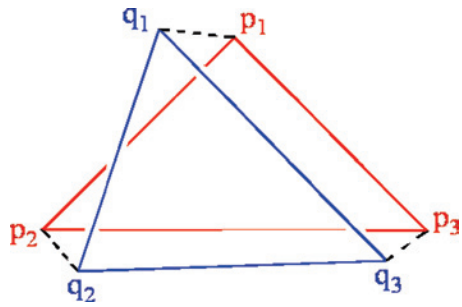

relative to an ideal polyhedron, P (Scheme 2), requires knowledge of the N vectors $\vec{q}_i$ describing the $3N$ Cartesian coordinates $\vec{q}_i$, as well as the corresponding vectors containing the coordinates $\vec{p}_i$ of the ideal polyhedron. The ideal shape is then rotated, translated, and scaled in such a way as to minimize the distance function in eq 3, which then gives the shape measure of the investigated structure, Q, relative to the ideal shape P as $S_Q(P)$.

$$S_Q(P) = \min\left[\frac{\sum_{i=1}^{N} |\vec{q}_i - \vec{p}_i|^2}{\sum_{i=1}^{N} |\vec{q}_i - \vec{q}_0|^2}\right] \times 100 \qquad (3)$$

In eq 3, $\vec{q}_0$ is the position vector of the geometric center of Q. According to the definition of CShM, if two shapes are identical, then $S_Q(P) = 0$, and the more different the shapes are, the larger the CShM values will be. Stereochemical studies of polyhedral structures having between four and nine vertices on the basis of CShM have been published by Alvarez et al.[56]

(56) (a) Alvarez, S.; Alemany, P.; Casanova, D.; Cirera, J.; Llunell, M.; Avnir, D. *Coord. Chem. Rev.*, and references cited therein. (b) Ruiz-Martínez, A.; Casanova, D.; Alvarez, S. *Chem. Eur. J.* **2007**, *14*, 1291.

Conclusion

In this paper, we report two new Cu^{II} linear trinuclear Schiff base complexes. DFT calculations based on the single-crystal X-ray structures have been used to model the exchange process, leading to the exchange integrals being qualitatively comparable to the experimentally determined values that reveal a moderate antiferromagnetic interaction. The relatively low exchange coupling in the case of complex **1** compared to that of complex **2** has been attributed to the small distortion toward TBP, which diminishes the contribution of the $d_{x^2-y^2}$ orbital, causing unfavorable overlaps of the magnetic orbitals. Additionally, CShM studies have been performed to quantitatively evaluate the loss of shape or symmetry, so as to estimate the degree of distortion in the Cu^{II} coordination polyhedron from an ideal polyhedron. Overall, a reasonable theoretical interpretation of the magnetic behavior shown by the complexes has been provided from the results of these studies.

Acknowledgment. S.T. gratefully acknowledges the Council of Scientific and Industrial Research, New Delhi, India, for the award of a Research Fellowship (CSIR Sanction No.09/096(0519)/2007-EMR-I). J.C. is thankful to the University Grants Commission, New Delhi, India, for a Senior Research Fellowship. Spanish (Grants CTQ2006-01759/BQU and CTQ2005-08123-C02-02/BQU) and Catalan (Grants 2005SGR-00593 and 2005SGR-00036) financial support is also acknowledged. J.T. is grateful to the Centre de Computació de Catalunya (CESCA), with a grant provided by Fundació Catalana per a la Recerca (FCR) and the Universitat de Barcelona.

Supporting Information Available: X-ray crystallographic files including the structural data for complexes **1** and **2** in CIF format. This material is available free of charge via the Internet at http://pubs.acs.org.

IC8001459